CARBON TRUST

Offshore Wind Accelerator

Fibre Optic Cable Protection Assessment

Induced voltage modelling

EnBW equinor Ørsted RWE SCOTTISHPOWER RENEWABLES sse Renewables VATTENFALL

Contents

The Offshore Wind Accelerator 1

Acknowledgements 1

1. Executive summary 2

2. Cables 3

3. Modelling 4

    3.1 Background 4

    3.2 Induced voltage 6

        3.2.1 Load current 6

        3.2.2 Capacitive currents 9

    3.3 Semi-conductive sheaths 11

    3.4 Power dissipation and temperature 16

    3.5 Corrosion 26

4. Known failures 29

5. Discussion 30

6. Conclusions 32

7. References 33

The Offshore Wind Accelerator

The Offshore Wind Accelerator (OWA) is the Carbon Trust's flagship collaborative research, development and deployment programme. The joint initiative was set up between the Carbon Trust and nine offshore wind developers in 2008, with the aim to reduce the cost of offshore wind to be competitive with conventional energy generation, as well as provide insights regarding industry standard (and best practice) health and safety requirements.

The current phase involves participation and funding from eight international energy companies: EnBW, Equinor, Ørsted, RWE, ScottishPower Renewables, Shell, SSE Renewables, and Vattenfall Wind Power, who collectively represent 75% of Europe's installed offshore wind capacity. This project also received partial funding from the Scottish Government.

Acknowledgements

This document was produced on behalf of the Offshore Wind Accelerator by RINA Tech UK Ltd, with technical review by the Offshore Wind Accelerator Cables Technical Working Group.

With a history going back 150 years, the RINA Group is a global corporation that provides engineering and consultancy services, as well as testing, inspection and certification.

1. Executive summary

This report describes the calculations and modelling carried out to assess the effectiveness of using semi-conductive sheaths and high resistance metallic parts in the fibre optic cable (FOC) to reduce the risk of failures due to interaction between the FOC and the power cores. The modelling has been based on the work by T. Kvarts (Kvarts, 2019) and J. Karlstrand (Karlstrand, 2019) with some additional developments.

Both papers conclude that the use of FOCs with high resistance metallic parts, a stainless steel tube, and a sheath with a resistivity of no more than 1000Ω·m will minimise any risk of damage to the FOC leading to failure of the power cores. The studies that have been carried out generally support this view.

An unarmoured design with just a small diameter stainless steel tube would result in less heat being generated at any break in the FOC than an armoured design. However, an unarmoured design will have less mechanical strength and hence would be more susceptible to damage during manufacture, load-out and installation than an armoured design. Therefore a design with stainless steel armour is proposed.

It has been concluded that where the sheath of an FOC has a resistivity of no more than 1000Ω·m and the metallic parts consist of a small diameter stainless steel tube to contain the fibres, and stainless steel wire armour, the heat generated at a break in the FOC will not be sufficient to damage the power cores.

Irrespective of the design of the FOC, any break in the metal tube water barrier will result in moisture ingress to the fibres. This will degrade the fibre performance. Thus, even if the fibres remain intact when the break occurs, they will not remain functional for the expected life of the export cable.

The possibility of AC corrosion of the stainless steel components has been considered. Published literature on AC corrosion is primarily concerned with AC corrosion of buried steel pipelines where there is a defect in the coating. The rate of corrosion is related to the current density at the defect. Thus, it is related to the driving voltage and the size of the defect. For a 1cm² defect in the sheath of an FOC, AC corrosion of the stainless steel would not be expected. However, corrosion testing with small defects/damage would be required to provide firm conclusions on the risk of AC corrosion in seawater.

It is also concluded that all of the metallic parts of the FOC have to be earthed at both ends and either earthed or made electrically continuous at any joints. Also, the use of an insulating adhesive between the metal parts and the sheath of the FOC must be avoided.

2. Cables

The cables considered in this report are three-core, high voltage (HV), cables incorporating one or more FOC, Figure 1.

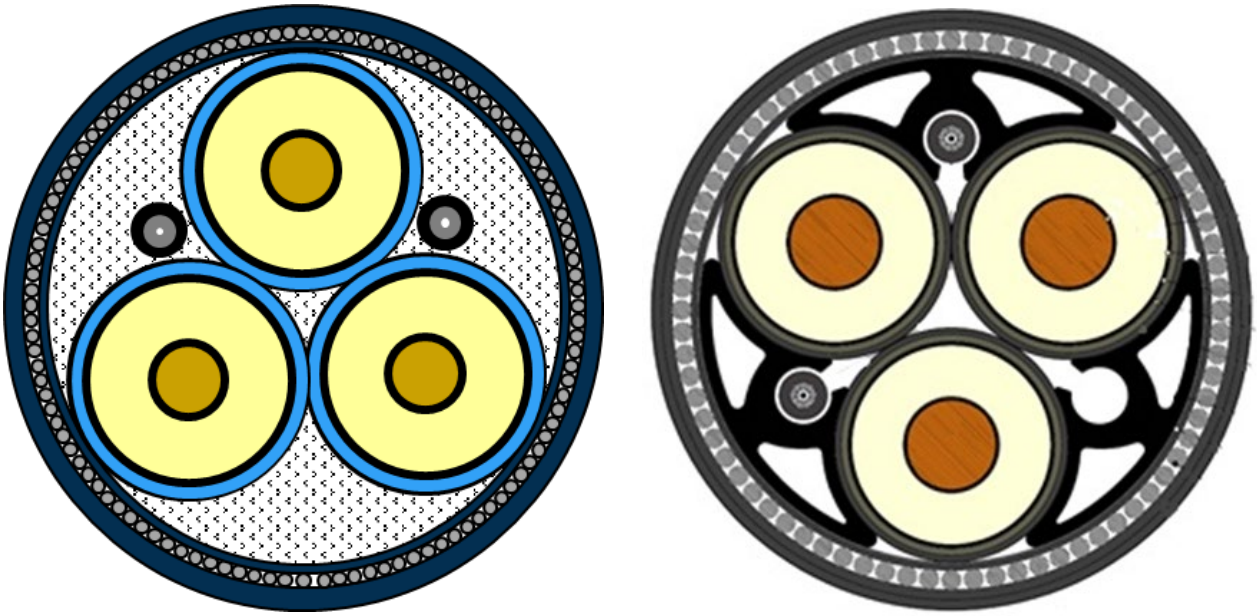

Figure 1: Cable designs

The power cores have a metallic sheath, usually lead, which is covered by an extruded, semi-conductive protective layer. The cables have one or more FOCs which are held in the fillers between the power cores. The fillers may be polypropylene rope or extruded sections. The cable fillers will become flooded with seawater.

3. Modelling

3.1 Background

The three-core submarine cable failures that the author has some details of, which have been attributed to interaction between the FOC and the power cores, broadly fall into two categories. One where the fibres were enclosed in a relatively low resistance metal tube and the tube is believed to have fractured leading to arcing between the parted ends of the tube. For this situation, the energy available due to the induced voltage and current in the tube was considered to be sufficient to damage the power cores. The second category relates to FOCs with aluminium wire armour around a stainless steel tube containing the fibres. For this design it appears that there was corrosion of the armour wires due to water ingress via a pin-hole or mechanical damage, and the corrosion was accelerated by the presence of an AC voltage. The localised loss of the armour wire led to localised overheating and failure of a power core.

There is also a third design of FOC where the fibres are within a small diameter stainless steel tube, without armour. Although the author is not aware of any power cable failures associated with this design, there have been instances where the stainless steel tube was found to have fractured. The author is not aware of the full details of this incident but it is believed that the breaks were found after the cable was laid but before it went into service.

The risk of damage to a power core due to interaction with a break in an FOC can be minimised if the design of the cable is such that the energy available at the break is not sufficient to degrade the surrounding materials. The modelling covered in this report is aimed at determining the conditions required to minimise the energy at a break in the FOC.

There are two ‘sources’ of induced voltage on the metallic parts of the FOC. These are the induced voltage due to the load current in the power cores, and the induced voltage due to capacitive charging currents in the power cores.

In an installed cable system, the metallic parts of the FOC should be bonded to earth at both ends of the cable and are likely to be bonded to the sheaths of the power cores and the armour of the cable at any joints. Where the FOC is bonded at both ends, the induced voltage due to the load current will drive a circulating current through the FOC. This effectively reduces the voltage on the FOC, due to the load current, to zero. However, if the continuity of the metallic parts of the FOC is broken there will be a standing voltage across the break. This voltage has to be assessed to determine whether it will drive sufficient current across the break, and to the power cores, to generate temperatures that could damage the power cores.

The load current is uniform over the length of the cable and hence the induced voltage it causes is uniform per unit length. However, the capacitive charging current is not uniform over the length of the cable and hence the induced voltage it causes is not uniform per unit length. Because of this there will be a standing voltage on the metallic parts of the FOC, even when it is bonded to earth at both ends. This standing voltage will be at a maximum at the mid-point of the cable run. Although this voltage is expected to be considerably lower than that due to the load current, it will

be present in a correctly installed system and could lead to accelerated corrosion of the metallic parts of the FOC if the sheath is breached.

Where the FOC has an insulating sheath the induced voltage on the FOC will be at a maximum. The use of a semi-conducting sheath allows some leakage current to flow through the sheath and this will reduce the standing voltage on the metallic parts of the FOC. The effect of the conductivity of the sheath has been modelled by both T. Kvarts and J. Karlstrand. Both calculation methods have been reviewed and, although there are some minor differences in the results from the two methods, both are considered to be appropriate.

Both T. Kvarts (Kvarts, 2019) and J. Karlstrand (Karlstrand, 2019) have considered three similar designs of FOC. The designs shown in Figure 2 have been taken from the paper by J. Karlstrand.

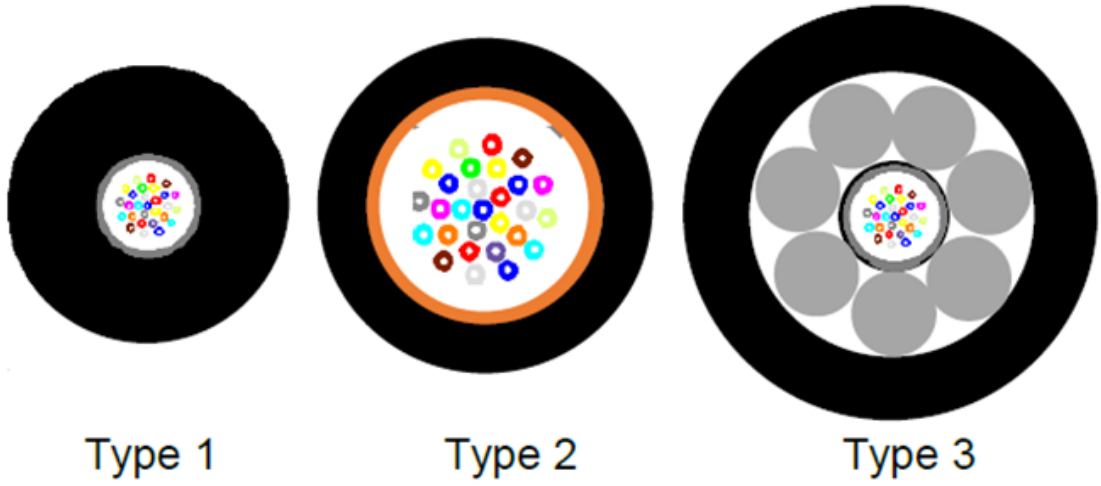

Figure 2: Designs of FOC

All three designs could have an insulating or semi-conductive sheath. The principal difference between the designs from the point of view of their electrical performance is the resistance of the metallic layers. The resistances used in both studies are shown in Table 1.

Table 1: Resistance of metallic components of FOC

	Resistance Ω/km		
Paper	Type 1	Type 2	Type 3
T. Kvarts	400	1.0	30
J. Karlstrand	258	1.78	0.57

Although both authors have chosen similar designs, it is clear that there is a significant difference in the properties chosen for Type 3. The difference is that T. Kvarts has selected stainless steel wire armour and J. Karlstrand has used aluminium wire armour. Both options are considered valid. For the examples in this report, the resistances given in Table 2 have generally been used.

Table 2: Resistance of metallic components of FOC

Resistance Ω/km		
Type 1 – Stainless steel tube only	Type 2 – Copper tube only	Type 3 – Stainless steel tube with SS armour
300	1	30

3.2 Induced voltage

3.2.1 Load current

For an FOC in a three-core cable, two currents which will generate induced voltage need to be considered: load current and capacitive charging current.

If the FOC has an insulated sheath and is only earthed at one end, with the cable carrying a balanced three phase load, then the induced voltage due to the load current at the open circuit end is given by:

$$V_{oc} = I \frac{1.2\mu_0\omega}{2\pi} ln\left(\frac{s_1}{s_2}\right) L$$

Where:

I	Load current, A
L	Cable length, m
V_{oc}	Induced voltage due to load current, V
μ_0	Permeability of free space, H/m
w	Angular frequency
s_1	Centre to centre distance between furthest conductor and FOC
s_2	Centre to centre distance between closest conductors and FOC

The factor 1.2 is included to take account of the effect of steel wire armour on the magnetic field within the cable.

In the presentation of the paper by delivered by T. Kvarts, at Jicable 2019, it was demonstrated that for the FOC in its usual position, in the interstices of the cable close to the power cores, the ratio s_1/s_2 is close to 2. This has led to the approximation that the induced voltage in an insulated, single-point bonded FOC, due to the load current, can be taken to be 50V/km/kA.

This approximation has been examined by considering the two extreme positions for the FOC, as shown in Figure 3.

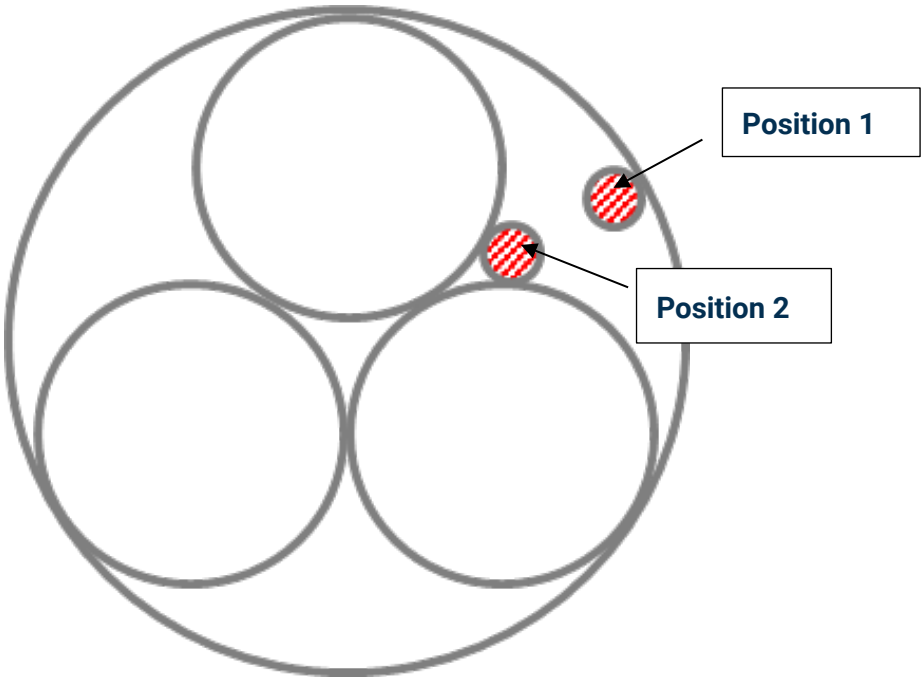

Figure 3: FOC positions

The induced voltage has been calculated for a range of power core diameters between 50mm and 100mm and a range of diameters of the FOC between 10mm and 20mm. For a load current of 1000A the calculated FOC voltages were between 45V/km and 52V/km. The lower voltages were where the FOC was furthest from the power cores.

The normal position for an FOC in a three-core submarine cable is close to the power cores, shown as Position 2 in Figure 3. Thus it is considered that, from the point of view of the possible interaction between the FOC and the power cores, it is appropriate to take the ratio s_1/s_2 as 2 and the induced voltage as 50V/km/kA. This is applicable to both array and export cables as well as other three-core subsea cables operating at any voltage, including 33, 66, 132 and 220kV.

Where the FOC is bonded to earth at both ends, the circulating current is such that the voltage is effectively zero over the whole length of the FOC. The circulating current, I_{cc} is given by:

$$I_{cc} = \frac{V_{oc}}{R_{FOC}}$$

Where:

R_{FOC}	Resistance of metallic parts of FOC, Ω/m.

Because both the resistance of the metallic parts of the FOC and the induced voltage are proportional to the length of the cable, the current flowing in the FOC is independent of length. This assumes that the resistance to earth at both ends of the FOC is negligible. The induced current is directly proportional to the load current in the power cores. For the examples of FOC design used by Kvarts and Karlstrand the current in the metallic parts of the FOC for a load of 1000A in the power cores, taking the ratio s_1/s_2 as 2, are given in Table 3.

Table 3: Current in FOC

Paper	Circulating current, A		
	Type 1	Type 2	Type 3
T. Kvarts	0.125	50	1.7
J. Karlstrand	0.194	28	88

If there is a break in the metallic parts of the FOC the heat generated at the break is proportional to the square of current flowing across the break. This current cannot be greater than the circulating current in the FOC and hence designs with lower circulating currents are at a lower risk than those with high circulating currents.

It is important that the metallic parts of the FOC are terminated in a manner that will not result in overheating, due to the circulating currents, at the bonding points. Where an FOC has both a stainless steel tube and armouring then both parts must be bonded.

Although the induced voltage due to load currents is not of concern for an intact and correctly bonded FOC it is of concern if there is a break in the continuity of the metallic parts. The voltage to earth, or the sheath of the power cores, at each side of the break will be a function of the distance from the break to the earthed ends of the FOC. However, the voltage across the break is independent of the position of the break, Figure 4.

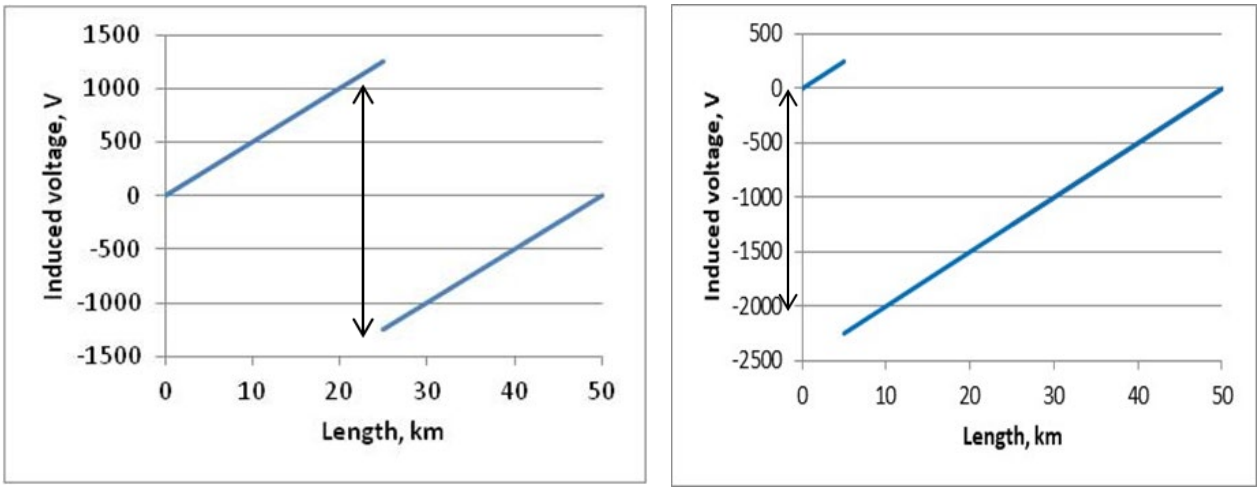

Figure 4: Voltage across break in FOC

3.2.2 Capacitive currents

The induced voltage due to the load current will effectively be zero with the metallic parts of the FOC bonded at both ends. However, because the charging current in the power cores of the cable is not uniform along its length the induced voltage in the FOC due to the charging current will not be zero.

The equation developed by Kvarts for the induced voltage, at any position along the cable, due to charging current for an FOC with an insulating sheath, can be written as:

$$V_{cx} = \frac{1.2\mu_0\omega}{2\pi} ln\left(\frac{s_1}{s_2}\right) \cdot (2\pi fCV)x \cdot 0.5(L - x)$$

Where:

C	Capacitance of power cable core, F/m
L	Cable length, m
V	System phase voltage, V
f	Frequency, Hz
x	Distance from end of cable, m

This equation is applicable to FOCs with an insulating sheath, which applies irrespective of the origin of the charging current.

An example of the profile of the induced voltage due to the charging current in a 220kV export cable is given in Figure 5.

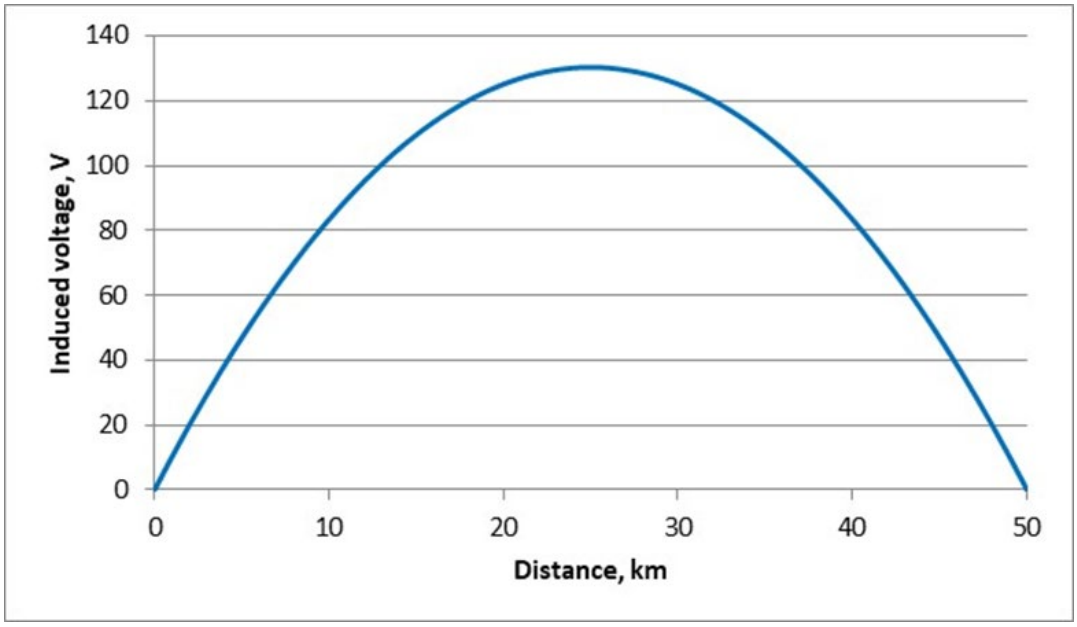

Figure 5: Induced voltage due to charging current

The maximum induced voltage occurs at the mid-length of the cable and hence the maximum induced voltage is given by:

$$V_{cx} = \frac{1.2\mu_0\omega}{2\pi} ln\left(\frac{s_1}{s_2}\right) \cdot (2\pi fCV) \cdot 0.125L^2$$

Using the same approximation, that s_1/s_2 can be taken to be equal to 2, as was used to derive the approximation that the induced voltage due to load current as 50V/km/kA, the equation becomes:

$$V_{cx} = \frac{50}{1000 \cdot 1000} \cdot I_C \cdot 0.125L^2$$

Where:

I_c	Capacitive charging current, 2πfCV, A/m

The capacitive charging current is a function of the cable design and the phase voltage. Charging currents for typical export and array cables are given in Table 4.

Table 4: Typical capacitive charging currents

System voltage, kV	A/km
33	1.5
66	2.5
132	5
220	8

For a 50km long export cable, the maximum induced voltage on the metallic parts of an FOC would be approximately 78V on a 132kV system and 125V for a 220kV system. Array cables are considerably shorter than export cables and operate at lower voltages, hence the induced voltage will be lower. For a 1km long 33kV array cable, the maximum induced voltage in the metallic parts of the FOC would be of the order of 0.009V, and for a 2km long 66kV system approximately 0.07V.

The much lower induced voltage on the FOC in array cables indicates that they are unlikely to suffer from significant AC corrosion in the event of damage to the sheath of the FOC.

3.3 Semi-conductive sheaths

One option that has been proposed to reduce the risk of failures due to interaction between the power cores of a subsea cable and the FOC is to use semi-conductive sheaths on the FOC. Semi-conducting sheaths are commonly used on the power cores of three-core export cables to minimise any voltage difference between the lead sheaths of each core. Semi-conducting sheaths have also been used on the FOC in some designs of export cable.

Where the FOC has a semi-conducting sheath there will be leakage current through the sheath and this will reduce the voltage on the metallic parts of the FOC to less than that with an insulating sheath. The magnitude of the reduction is a function of the resistivity of the sheath material. The lower the resistivity the greater the reduction.

Both Kvarts and Karlstrand have considered the effect of a semi-conducting sheath on the induced voltage on the FOC. In the work by Kvarts, for the effect of the semi-conducting sheath, the equations have been solved using a commercial circuit simulation software package. In the work by Karlstrand, an approximate analytical solution has been obtained using transmission line theory that was originally developed for long distance communications systems. The basic equation for

the voltage at a point along a transmission line where the receiving end is short-circuited is given in the book Electric – Circuit Theory by Benson and Harrison (Benson & Harrison, 1959) as:

$$V_x = V_s \frac{sinh(\gamma(L-x))}{sinh(\gamma L)}$$

Where:

V_x	Voltage at distance x from source
V_s	Source voltage
L	Length of line
g	$\sqrt{(R + j\omega L)(G + j\omega C)}$
C	Capacitance per unit length
G	Conductance, of 'insulation', per unit length
L	Inductance per unit length
R	Resistance per unit length
ω	Angular frequency

In calculating the conductance of the sheath of the FOC it is assumed that there is an earth plane at the outer surface of the sheath of the FOC: seawater. In this case G is given by:

$$G = \frac{2\pi}{\rho \, ln\left(\frac{d_o}{d_i}\right)}$$

Where:

d_i	Inner diameter of FOC sheath
d_o	Outer diameter of FOC sheath
r	Resistivity of sheath material

The basic equation has been modified by Karlstrand for application to the FOC where the voltage is a function of the distance along the FOC and the resistance of the FOC is many times greater than its reactance.

Because it offers an analytical solution, the work by Karlstrand has been adopted for this report. It is recognised that the assumptions in the solution offered by Karlstrand result in a simplification that affects the accuracy of the calculations that is not present in the approach taken by Kvarts. However, it is considered that the simplification does not result in errors of such a magnitude as to invalidate the results from the Karlstrand approach.

The equation given for the voltage, V_{cx}, due to capacitive currents, at any point along the FOC is:

$$V_{cx} = \frac{1.2\mu_0\omega}{2\pi} ln\left(\frac{s_1}{s_2}\right)\frac{\omega^2 CV}{\gamma^2}\left(1 - \frac{sinh\big(\gamma(L-x)\big) + sinh(\gamma x)}{sinh(\gamma L)}\right)$$

Where:

g	$\sqrt{R_{FOC}G}$ For an FOC with a semi-conductive sheath
G	Conductance of FOC sheath l, 1/Ω·m

For a correctly installed FOC which is solid bonded the maximum voltage appears at the mid-length of the cables and the equation is simplified to:

$$V_{cmax} = \frac{1.2\mu_0\omega}{2\pi} ln\left(\frac{s_1}{s_2}\right)\frac{\omega^2 CV}{\gamma^2}\left(1 - \frac{1}{cosh\left(\gamma\frac{L}{2}\right)}\right)$$

These equations show that the voltage on the FOC is a function of both the resistance of the metallic elements and the resistivity (conductivity) of the sheath material.

The voltage profiles for a 50km, 132kV export cable with different resistances of the metallic parts are shown in Figure 6 to Figure 8. In these examples the resistivity of the sheath of the FOC has been taken to be 10^9, 10^6 and 10^3Ω·m respectively.

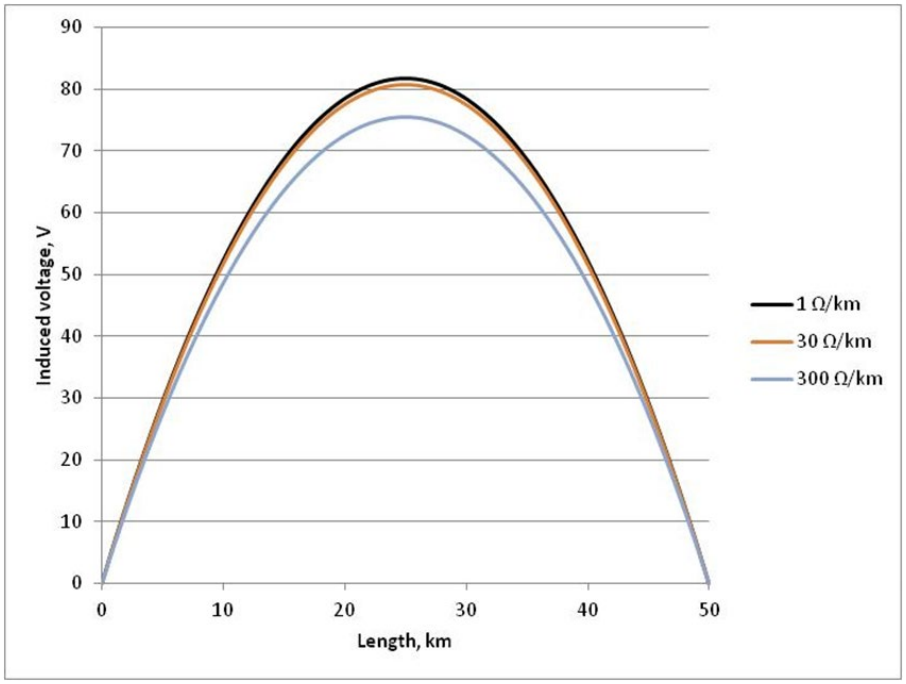

Figure 6: Effect of resistance of metallic parts - 109Ω·m FOC sheath

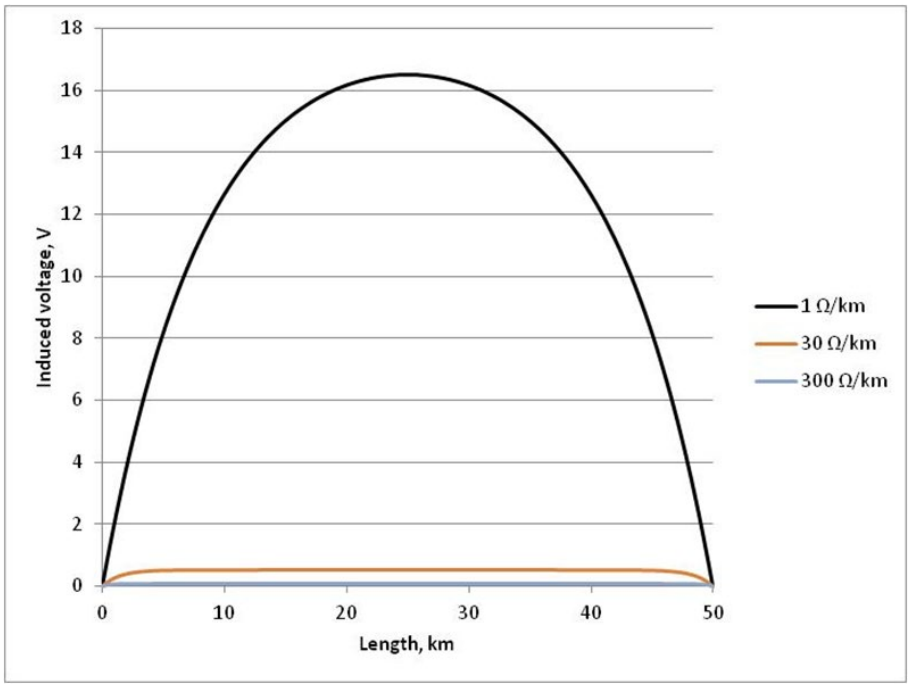

Figure 7: Effect of resistance of metallic parts - 10^6Ω·m FOC sheath

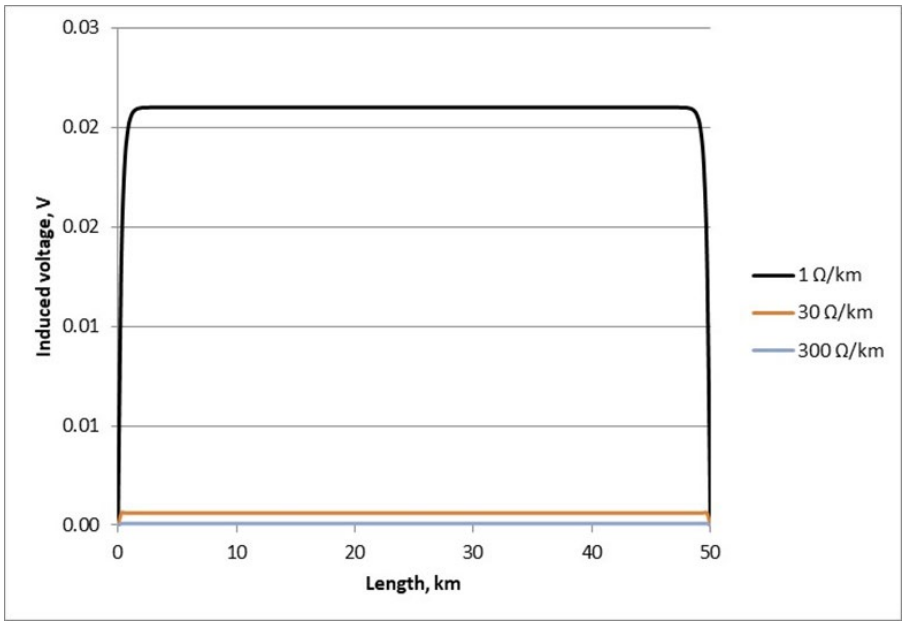

Figure 8: Effect of resistance of metallic parts – 10^3Ω·m FOC sheath

These plots show that, as expected, the resistance of the metallic parts of the FOC does not have a significant effect on the voltage on the FOC where the sheath has a relatively high resistivity.

In addition to the effect the resistivity of the FOC sheath has on the induced voltage due to capacitive charging currents in the power cores, it will also affect the induced voltage across a break in the metallic parts of the FOC.

The equation given by Karlstrand for the induced voltage, due to load current, at the open end of a single-point bonded FOC can be approximated to:

$$V_{oc} = I\frac{1.2\mu_0\omega}{2\pi}ln\left(\frac{s_1}{s_2}\right)\frac{tanh(\gamma L)}{\gamma}$$

Although this equation is not relevant for a correctly earthed FOC it can be used to calculate the voltage across a break. The voltage across a break in the metallic part of an FOC at the mid-length of a 50km, 132kV, export cable with a balanced load current of 1000A has been calculated for a range of resistances of the metallic parts and resistivity of the sheath material. The resistances used were: 300Ω/km for a stainless steel tube, 30Ω/km for a stainless steel tube with stainless steel armour wires and 1Ω/km for either a copper tube or a stainless steel tube with aluminium armour wires. The results of these calculations are given in Table 5. These results do not consider the current flow through any semi-conducting materials that surround the break. The actual voltages across a break where the sheath has a resistivity of less than 1000Ω·m will be considerably lower than those given.

Table 5: Voltages at break in FOC, V

Sheath resistivity, Ω·m	Resistance of metallic parts, Ω/km		
	300	30	1
	Voltages across break in FOC, V		
10^{12}	2611	2613	2613
10^{9}	1657	2405	2606
10^{6}	59	161	930
10^{3}	1.9	5.1	29.6

These values clearly show that with an insulating sheath on the FOC the resistance of the metallic parts has a negligible effect on the voltage that could appear across a break. However, if the resistance of the sheath is reduced to the order of 1000Ω·m there is a dramatic reduction in the voltage across a break. If the resistance of the metallic parts is of the order of 30Ω/km or more then the induced voltage across a break is very unlikely to cause tracking that could degrade the surrounding materials.

3.4 Power dissipation and temperature

For an FOC having a stainless steel tube and aluminium wire armour, ingress of seawater through damage to the sheath of the FOC is likely to result in corrosion of the aluminium wire armour. If the aluminium wire armour becomes open circuit over a short length the circulating current in the FOC will have to travel through the stainless steel tube only for a short length. Although the loss of a short section of armour wire will increase the resistance of the FOC in that area it will only have a small impact on the total resistance over the whole length of the FOC. Hence the change in the circulating current will be insignificant. Limited testing on a section of stainless steel tube from an FOC, in air, has shown that the temperature of the tube rapidly achieved in excess of 200°C with a current of 40A. Thus, it is clear that localised loss of aluminium armour due to corrosion will lead to temperatures that will cause degradation of the materials around the FOC.

The remainder of this section covers assessment of the temperature that may be achieved if there is a complete break in the metallic parts of an FOC but the sheath remains intact. The assessment considers the conditions that may exist when the metallic parts of the FOC have parted during manufacture or installation. If the temperature at the fault is very high, as a fault progresses when the cable is in service, it is expected that the sheath of the FOC at the break could become carbonised and as the conditions change the rate of deterioration will accelerate.

For an interaction between an FOC and the power cores of a subsea cable to occur there has to be sufficient heat generated at the break in the FOC to damage the power cores. In simple terms the heat generated at a break is given by I^2R, where I is the current across the break, or to the sheath of the power cores and R is the resistance at the break. However, when the voltage across a break is sufficiently high it is likely that there will be tracking and arcing across the break. The heat generated by arcing will be much greater than that calculated by simply considering the resistance across the break and the current flowing through it. The heat generated at a break could cause localised degradation of the sheaths of the power cores and FOC as well as the filler materials. The current flowing across the break cannot exceed the maximum circulating current in the metallic parts of the FOC (see Table 3).

Two types of break in the FOC are considered possible. One where the metallic part of the FOC has parted but the sheath is intact and the other where both the metallic parts and the sheath have parted. Given the difference between the elastic properties of the metallic parts and the sheath materials, it is considered that it is entirely plausible that the sheath can remain intact but continuity through the metallic parts has been lost. If the sheath of the FOC has parted then the area between the ends of the break will flood with seawater which will reduce the resistance across the break to a few ohms or tens of ohms, depending on the length of the break.

Where the metallic parts have broken and the sheath of the FOC remains intact current can flow across the break via the sheath, if the sheath is semi-conductive. If the sheath is insulating then the voltage across the break will be high (Table 5). A high voltage across the break is likely to lead to tracking across the inside surface of the sheath, carbonisation and arcing. No information is available on the tracking performance of the sheath material but it is clear that once arcing is initiated very high temperatures will occur and this will lead to rapid degradation of the surrounding polymers as well as melting of the lead sheath of the power cores.

With an insulating sheath the I^2R heat generated at a break will be a maximum when the resistance across the break is equal to the resistance of the metallic parts of the FOC. In this situation the current across the break will be half of the calculated circulating current in an intact FOC. The maximum heat generated at a break in a 50km submarine cable carrying 1000A and having an FOC with an insulating sheath and metallic parts having resistances of 300, 30 and 1Ω/km is given in Table 6. The values given assume that the induced voltage in the FOC is 50V/km/A.

Table 6: Heat generated with an insulated FOC

Resistance of metallic parts (Ω/km)	300	30	1
Circulating current with intact FOC, A	0.167	1.67	50
Resistance of intact FOC, Ω	15000	1500	50
Resistance across break, Ω	15000	1500	50
Current across break, A	0.083	0.83	25
Heat generated at break, W	104	1041	31250

The power dissipation at a break in an FOC with an insulated sheath is shown in Figure 9 as a function of the resistance across the break, as a percentage of the resistance of the metallic parts of the FOC, for a 50km long submarine cable.

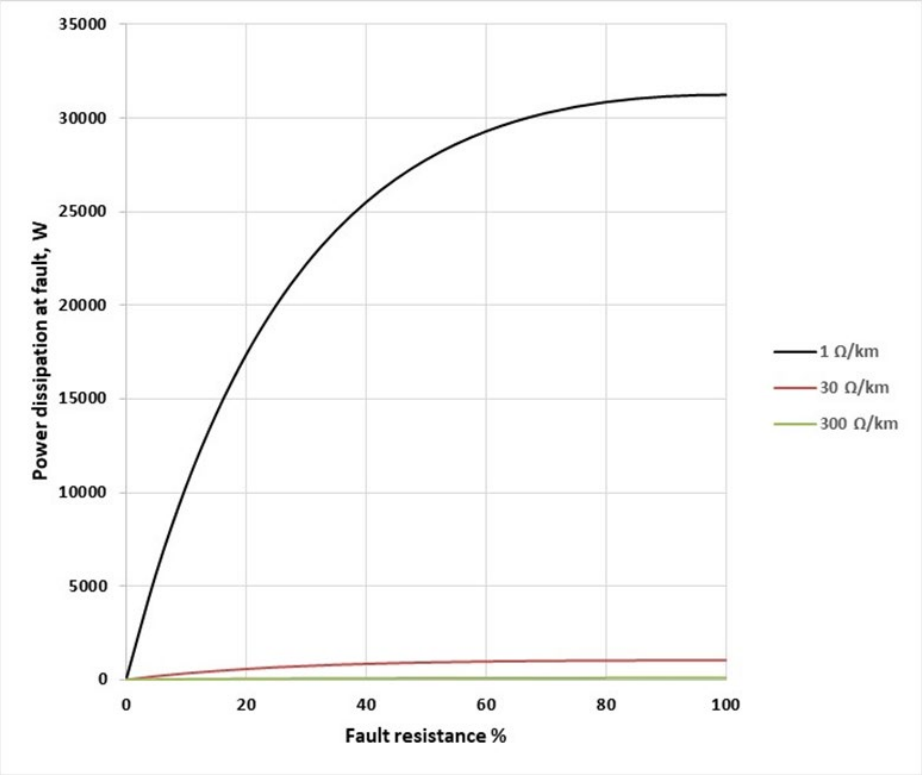

Figure 9: Power dissipation at break in FOC

With an insulating sheath the maximum heat that could be generated at a break is clearly sufficient to damage the FOC, irrespective of the resistance of the metallic parts of the FOC. However, the heat generated at a break is reduced with increasing resistance of the metallic parts of the FOC.

Where the FOC has a semi-conductive sheath current can flow longitudinally across the break along the remaining tube of semi-conductive sheath material, and radially through the sheath, filler materials and seawater within the export cable to the power cores and the cable armour (Figure 10). The current paths to the power cores and armour will be dependent on the design of the cable. In some designs the FOC is held in an extruded, shaped, filler which may be of an insulating or semi-conductive material. In other designs the interstices between the power cores are filled with rope fillers, often polypropylene, and the FOC is held within these fillers. The current flow to the power cores and armour will be through the semi-conductive sheath and other materials and hence this path is expected to have a considerably higher resistance than that through a short 'tube' of semi-conducting sheath straddling the break.

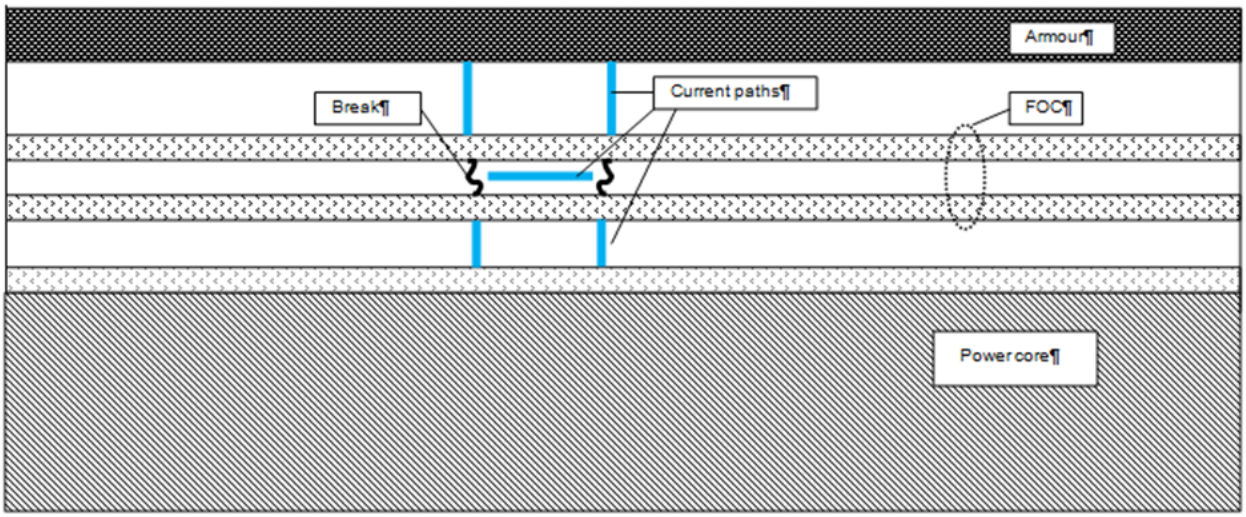

Figure 10: Sketch of current paths

The current flow across the break, directly through the sheath of the FOC, will be a function of the resistance of this path and the voltage across the break. This voltage will be the open circuit induced voltage over the whole length of the cable, irrespective of the position of the break. The current flow to the armour at each side of the break will be a function of the voltage on the FOC at each side of the break. Similarly, the current flow to the power cores will be a function of the voltage between each side of the break and the lead sheaths of the two adjacent power cores. This voltage will be affected by any residual standing voltage on the lead sheaths of the power cores, which should be minimised by the semi-conducting sheaths of the power cores. The resistance of the semi-conducting sheath of the power cores will also form part of the resistance in this current path.

The voltage on the metallic parts of the FOC at each side of the break will be out of phase (Figure 4). Thus, the currents flowing from each side of the break to the armour and power cores will be out of phase. If the distance between the ends of the break is small there will be some interaction between out of phase currents flowing to the armour and the power cores.

Because of the multiple factors involved in determining the current flow through the various paths it is not practical to reliably calculate the heat generated at a break in the metallic parts of an FOC with a semi-conducting sheath. However, in this paper Karlstrand offers a simplified equation which assumes that the current flows to an earth plane at the surface of the FOC, seawater. This equation is:

$$W = \frac{1}{2}(I_F)^2 \sqrt{\frac{R_F}{G_F}}$$

Where:

I_F	Circulating current that will flow in the FOC

This equation has been used to calculate the maximum power dissipation at a break in the FOC where a 50km submarine cable is carrying 1000A (Table 7).

Table 7: Maximum power dissipation at a break

FOC design		Type 1	Type 2	Type 3	Type 1	Type 2	Type 3
Sheath resistivity	Ω·m	10^3	10^3	10^3	10^6	10^6	10^6
Resistance of FOC	Ω/km	300	1	30	300	1	30
Power dissipation at break	W	0.07	346	1.87	2.3	6071	53

A 3D finite element model has been used to provide an indication of the temperature rise of the FOC and surrounding materials for the power dissipations given above. The cable modelled is a generic 132kV cable. Standard values were used for the thermal resistivity of the majority of the cable components. The thermal resistivity of the fillers with seawater filling the voids has been taken as 2.5K·m/W. In this model it has been assumed that the heat is generated in the sheath of the FOC at a 5mm wide break in the metallic components.

For the model, the cable was considered to be buried in the seabed at a depth of 800mm and the thermal resistivity of the seabed was taken to be 0.8K·m/W.

The 3D model was used to calculate the temperature rise of the FOC and the lead sheaths of the power cores due to the heat generated at the break in the FOC. Hence, the outer surface of the model was set as an isotherm at 0°C. An adiabatic boundary was set at both ends of the 0.5m long section of cable that was modelled. The layout of the model is shown in Figure 11 with the portion generating heat shown in green.

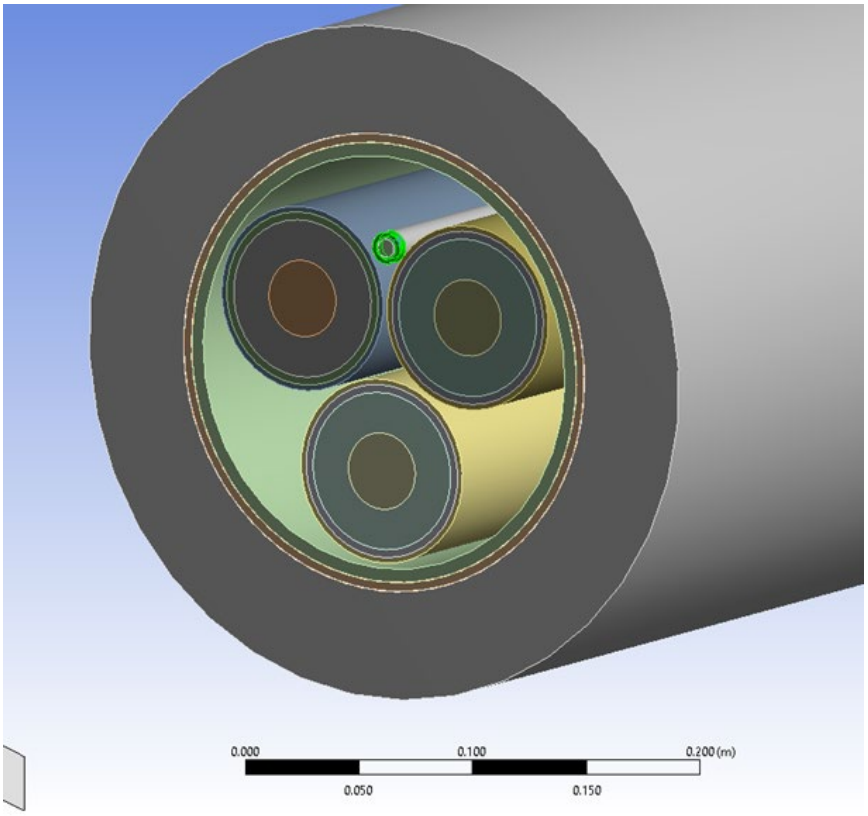

Figure 11: 3D Finite element model

The model was run for a range of power dissipations and different conductivities of the metallic part of the FOC to represent a stainless steel tube, stainless tube with armour and a copper tube.

The temperature plot around the FOC for the run with the FOC having a stainless steel tube and stainless steel wire armour with a power dissipation of 2W at the fault is shown in Figure 12. The temperature profile along the FOC is shown in Figure 13. This temperature profile confirms that the 0.5m long section modelled was long enough to minimise end effects. It also shows that the length of the FOC with a significant temperature rise is less than 100mm each side of the fault.

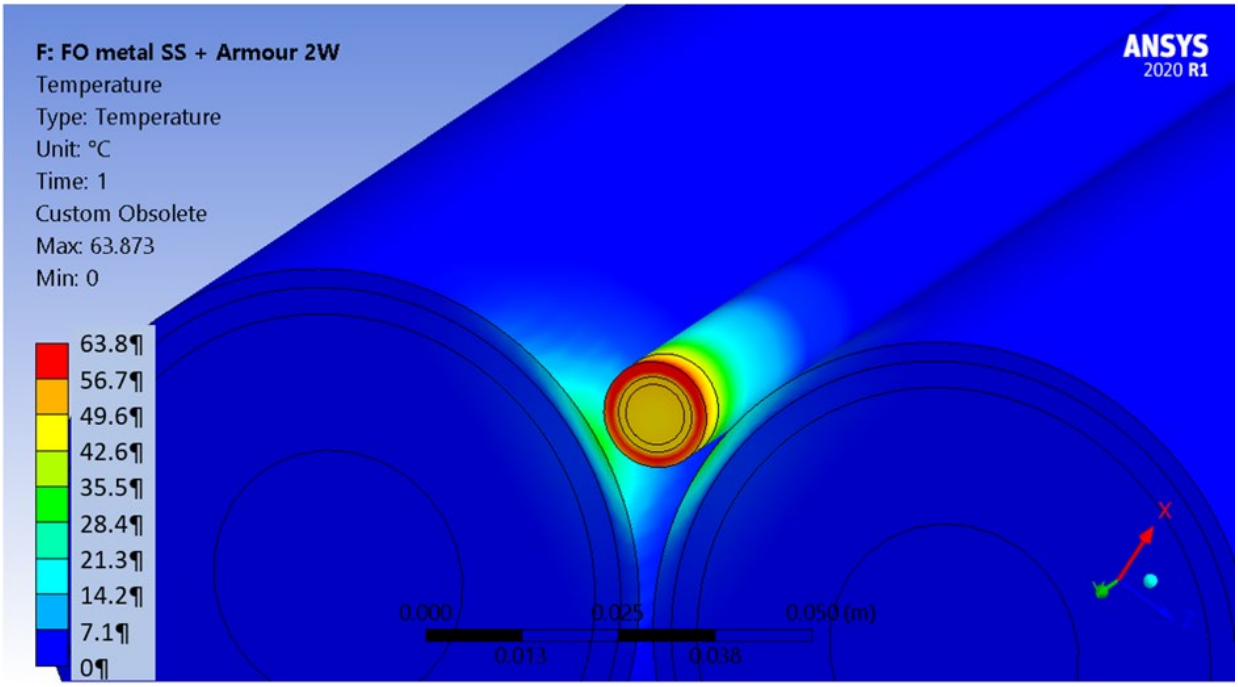

Figure 12: Temperature plot around FOC

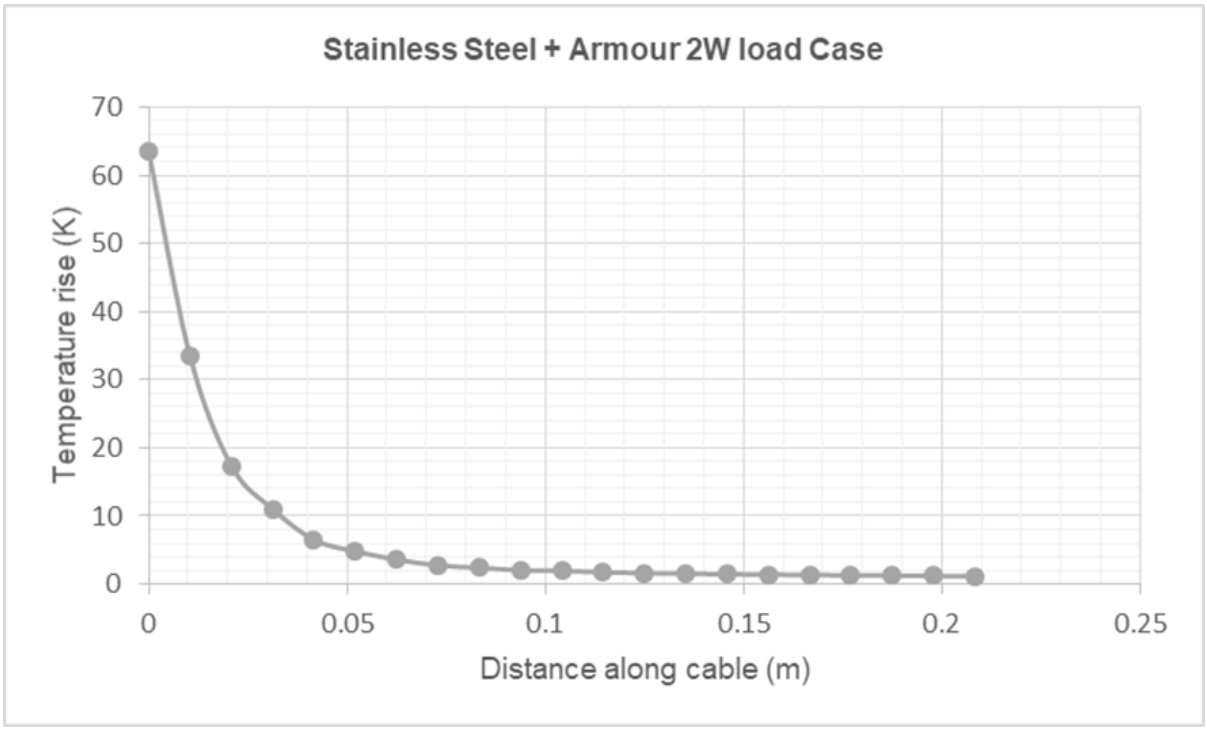

Figure 13: Longitudinal temperature rise plot

The temperature rises of the FOC and the adjacent lead sheath of the power cores for the power dissipations given in Table 7 are given in Table 8. The temperature rises for the design having a copper tube and a sheath resistivity of $10^6\Omega\cdot m$ were not calculated because of the very high temperatures found with this design with a sheath resistivity of $10^3\Omega\cdot m$.

Table 8: Estimated temperature rise at break in metallic part only

	Units	Type 1 Stainless tube	Type 2 Copper tube or SS tube and Al armour	Type 3 Stainless tube and stainless armour	Type 1 Stainless tube	Type 2 Copper tube or SS tube and Al armour	Type 3 Stainless tube and stainless armour
Sheath resistivity	Ω·m	10^3	10^3	10^3	10^6	10^6	10^6
Power dissipation at break	W	0.07	346	1.87	2.3	6071	53
Temperature rise of FOC sheath	K	3.3	6301	59.6	110	NA	1690
Temperature rise of power core lead sheath	K	0.2	710	5.3	7.3	NA	150

The modelling has confirmed that the temperature rise of the FOC and the lead sheaths of the power cores is directly proportional to the power dissipation at the break. The temperature rise per watt power dissipation is given for two designs in Table 9.

Table 9: Temperature rise per Watt

Design	FOC	Lead sheath
Stainless steel tube only	47.8K/W	3.2K/W
Stainless steel tube with armour	31.9K/W	2.9K/W

These results are the temperature rise due to heat generated at the break. To obtain the actual temperature it would be necessary to add the temperature rise due to the load current and ambient temperature. For a 132kV export cable operating at its maximum permitted conductor temperature of 90°C the temperature of the lead sheath would be expected to be approximately 75°C. However, for an export cable this temperature would only be achieved at the most thermally onerous part of the route, with the cable carrying its full rated current. Thus, the temperature of the lead sheath in installed export cables is expected to be well below 75°C. Where the author has seen records from distributed temperature monitoring systems, in export cables, the maximum temperature seen was approximately 50°C with temperatures of 35°C being more common over the length of the route.

These results indicate that for FOCs with just a stainless steel tube and a semi-conductive sheath having a resistivity of up to $10^3\Omega\cdot m$ no damage would be expected due to the heat generated at a break in the metallic parts only. The temperature rise at a break in a low resistance copper tube would clearly cause damage to the power cores irrespective of the resistivity of the sheath. Where the FOC has stainless steel armour the calculated temperature rise at the lead sheath will not result in degradation of the lead sheath or the underlying XLPE insulation, with a sheath resistivity of up to $10^3\Omega\cdot m$. However, the maximum temperature at the break in the FOC could reach approximately 135°C in an extreme case, although temperatures of around 110°C are considered more likely. Such temperatures are above the normal operating temperature of the FOC and the adjacent filler materials and will lead to accelerated ageing of the materials. However, they will not lead to carbonisation of the material and degradation that could lead to damage to the power cores.

Any break in the metal tube containing the fibres will lead to moisture ingress around the fibres which will degrade the performance of the optical fibres. Accelerated degradation of the sheath of the FOC due to the temperatures generated at a fault will accelerate the rate of moisture ingress. Where the metallic parts of the FOC and its sheath both break the current paths will be slightly different. The break will be flooded with seawater. The resistivity of seawater can be taken as $0.2\Omega\cdot m$, hence the resistance across the break will be considerably lower than without a break in the sheath. Also, the path to the power cores and armour will have a lower resistance. A finite element model was used to estimate the resistance between the metallic parts of the FOC and the power cores and armour. In this model a voltage was set on the FOC, and the armour and lead sheath of the power cores were set at zero volts. The model used was one where the FOC was embedded in polypropylene fillers. The electrical resistivity of these fillers when flooded with seawater is not known. For the purpose of these calculations it has been assumed that the seawater occupies approximately 10% of the total volume of the fillers leading to a resistivity of ten times that of seawater: $2\Omega\cdot m$. The modelling was carried out for a sheath resistivity of $10^3\Omega\cdot m$.

The current path across the gap between the broken ends of the FOC has been modelled as a short rod of seawater having a diameter equal to the diameter over the sheath of the FOC.

For the situation where there is a 5mm gap at the break in the FOC and the FOC is embedded in polypropylene rope fillers, the finite element study showed that the current flow across the ends of the FOC was more than eight times that flowing to the power cores and armour. This was mainly due to the resistivity of the sheath of the power cores being high relative to the resistivity of sea water and the longer path to the armour. In calculating the temperature rise for this situation the current flow to the power cores has been ignored. The calculated temperature rises for this situation are given in Table 10.

Table 10: Estimated temperature rise at break in metallic part and sheath – rope fillers

FOC design		Type 1 Stainless tube	Type 3 Stainless tube and stainless armour
Sheath resistivity	Ω·m	10^3	10^3
Power dissipation at break	W	0.035	1.7
Temperature rise of FOC sheath	K	1.6	48
Temperature rise of power core lead sheath	K	0.1	4.1

Where the FOC is held in a groove in shaped extruded fillers (Figure 14) the current path from the FOC to the power cores and armour is more complex.

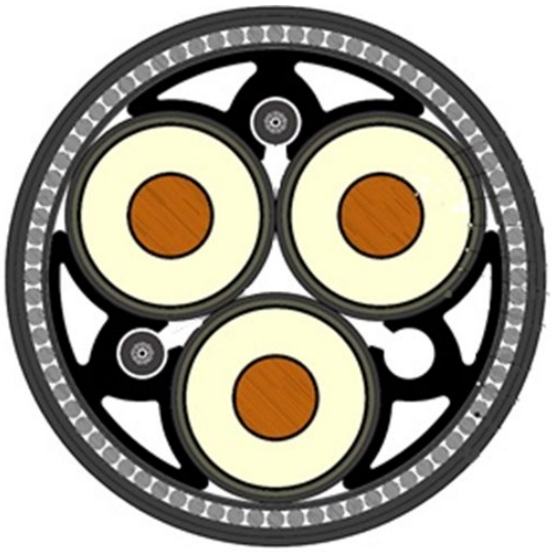

Figure 14: Example of extruded fillers

The extruded fillers may be insulating or semi-conductive. In either case the resistivity of the fillers will be much higher than that of the seawater that fills the voids – approximately 1000Ω·m compared to 0.2Ω·m. To provide an approximation of the current flow from a break in the metallic parts of the FOC to the lead sheath of the power cores and the armour, a finite element model was used where the resistivity of the 'filler' materials was taken to be that of seawater, 0.2Ω·m, therefore the effect of the extruded filler was ignored.

As expected the current flow was generally to the cable armour rather than the sheaths of the power cores, due to the resistivity of the semi-conducting sheaths being much higher than that of seawater.

The calculated power dissipation at a break in the FOC for the design with extruded filers was approximately 10% higher than that with polypropylene fillers. Thus, the temperature rise was approximately 10% higher than those given in Table 10. With the approximations made during the various stages of the calculations it is considered reasonable to conclude that the design of the fillers, polypropylene string or extruded sections, will not influence the outcome in the event of a break in the metallic parts of the FOC.

3.5 Corrosion

One of the initial phases of some the failures that have been identified was corrosion of the aluminium armour wires in the FOC. It is well known that the presence of an AC voltage on metalwork that is in water or buried in the ground can lead to accelerated corrosion. Studies that have been carried out generally cover the situation where a buried pipeline runs parallel to a transmission or distribution circuit such that there is an induced voltage in the pipeline. The calculation methods for determining the AC voltage for this situation are discussed in CIGRE TB 95 (TB 95 - Guide to the influence of high voltage AC power systems on metallic pipes, 1995) and are comparable with those used for calculating the induced voltage due to load current on an FOC with an insulating sheath. The effect of AC voltage on corrosion rates for steel pipes is given in BS EN 15280 (BS EN 15280 Evaluation of a.c. corrosion likelyhood of buried pipelines applicable to cathodically protected pipelines, 2013).

The steel pipelines covered by BS EN 15280 are taken to have an insulating coating and the risk of corrosion occurs where there is a defect or damage to the coating that exposes the steel. The standard indicates that if the current flowing between the pipe and the ground has a density of less than 30A/m² then corrosion due to the AC voltage is unlikely to occur. Thus, the risk of AC corrosion of steel is a function of the magnitude of: the induced voltage, the resistivity of the surrounding material and the area of steel that is exposed. An indication of corrosion rates for steel has been taken from a 1996 paper by R. Gummrow (Gummrow, 1996) and is shown in Figure 15.

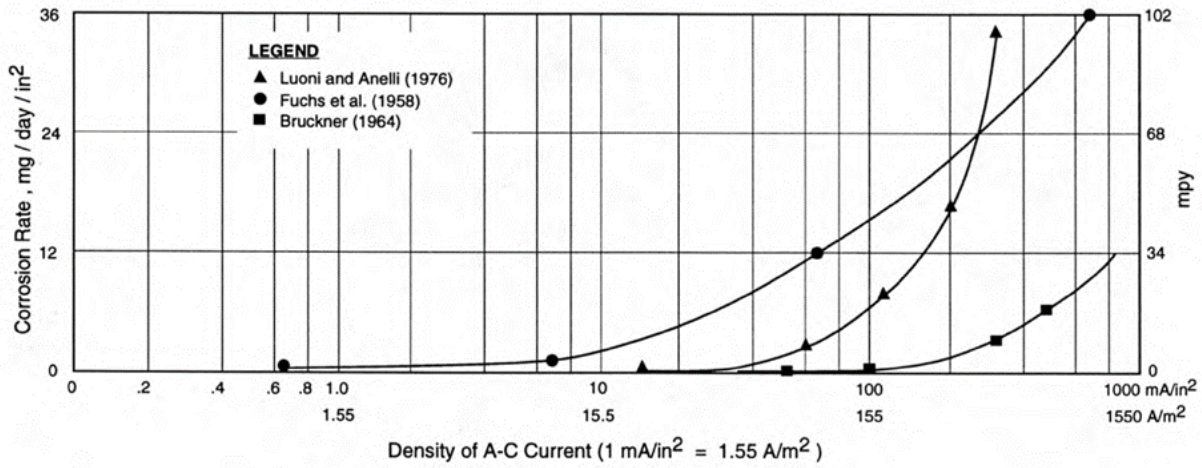

Figure 15: Steel corrosion rates under different conditions

The three curves represent different conditions. The work by Luoni and Anelli (Luoni & Anelli, 1976) was on galvanised steel in salt water, that by Fuchs on uncoated steel in salt water and that by Bruckner for uncoated steel in neutral soil. These results show that the 30A/m² is appropriate in neutral soil and galvanised steel in seawater but optimistic for uncoated steel in seawater.

Work carried out by W. French on AC corrosion of aluminium (French, 1973) proposes a critical current density of 0.5mA/in² (0.78A/m²) below which corrosion of the aluminium is not expected to occur. French reports that “the tests were run in a number of different soils and water having different pH, resistivity and chloride levels” but he does not state the effect of the different conditions. Figure 16 is an extract from the report by French which supports the 0.78A/m² limit.

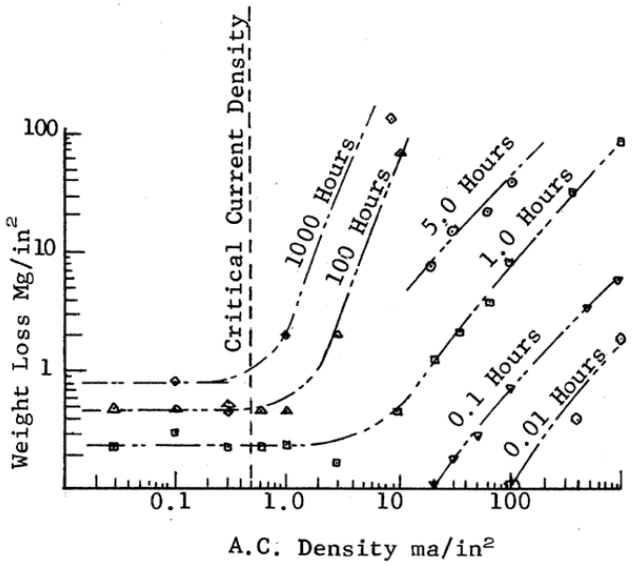

Figure 16: Aluminium corrosion rates

A number of studies have been carried out into AC corrosion of different grades of stainless steel in sea water. The published papers that have been reviewed do not give direct conclusions regarding a safe limit for current density. However, the test results indicate that 40A/m² is a reasonable limit for stainless steel in seawater. Results of tests carried out by B. Gustavsen on stainless steel pipes in seawater (Gustavsen, 2018) indicated negligible corrosion of the stainless steel at a current density of 100A/m², however the duration of the tests is not reported.

A literature search was carried out for published information on the AC current density required to cause corrosion of copper in seawater. No direct values were found but sufficient information was obtained to indicate that its performance is very much better than aluminium and no worse than that of galvanised steel and stainless steel.

For all of the above materials the limiting AC current density is the value below which corrosion would not be expected. As the driving voltage and hence current density increase, not only does the risk of AC corrosion increase, but so does the rate of corrosion. For current densities just above the accepted limits the rate of corrosion may be such that failure would not occur over the expected life of the cable.

The following equation is used for calculating the current density, A/m², at a defect (holiday) in the coating of a buried steel pipeline where there is an induced voltage:

$$I_{ac} = \frac{8V_{ac}}{\rho \pi d}$$

Where:

V_{ac}	Induced voltage, V
d	Diameter of circular defect, m
r	Soil resistivity Ω·m

In a pipeline the coating is expected to be bonded to the pipe and hence the area of the defect is the area of metal available for corrosion. If the sheath of an FOC is damaged such that the metallic parts are exposed to seawater then water will penetrate the FOC so that the area available for corrosion will be larger than the size of the damage. Because of this the above equation may not provide a reliable indication of whether the induced voltage on the metal parts of the FOC is likely to lead to corrosion in the event of sheath damage. In order to indicate the order of magnitude of the induced voltage that may lead corrosion of galvanised steel, stainless steel and aluminium the limiting voltage has been calculated for an exposed surface area of 1cm². The worst case is considered to be with the surrounding material being seawater having a resistivity of 0.2Ω·m. However, the current flow will also be through water logged fillers and semi-conducting materials. These paths may result in an effective resistivity that is higher than seawater alone hence the calculations have also been carried out for a resistivity of 2Ω·m. The results of these indicative calculations are given in Table 11.

Table 11: Indicative voltages for AC corrosion

Property	Galvanised steel	Stainless steel	Aluminium
Limiting current density, A/m²	30	40	0.78
Resistivity 0.2Ω·m	0.027	0.035	0.0007
Resistivity 2Ω·m	0.27	0.35	0.007

Although the above voltages are only indicative it is clear that aluminium armour wires should be avoided if there is a risk that the sheath of the FOC could be damaged.

4. Known failures

The author is aware, either fully or partially, of the details of the failures of a number of HV subsea cables where the cause of the failure has been attributed to an interaction between the FOC and the power cores. The models described above have been used to determine the voltages that could have existed on the FOCs. In all cases the calculated voltages were high enough to cause AC corrosion of the metallic parts for the FOC if its sheath had been breached. Also, the currents and voltages where the metallic parts of the FOC had parted were such that sufficient heat could be generated to carbonise the materials around the break and cause damage to the power cores.

Where the failures seen were due to a mechanical break in the FOC tube rather than corrosion of aluminium armour wires, the thermal degradation of the FOC sheath only extended a short distance to each side of the fault. This is consistent with the extent of the longitudinal heat transfer shown by the finite element model.

None of the failures (where the author is aware of sufficient details) involved a high resistance, unarmoured, design of FOC with a stainless steel tube. Although several failures involved FOCs with a semi-conducting sheath, the effective resistivity of the sheaths was considerably higher than 1000Ω·m.

In a number of cases the earthing of the metallic parts can be described as ‘uncertain’ for at least part of the life of the cable and in one case the FOC was known to be unearthed at one end.

From the review of known failures, the conclusions that the failures were due to interaction between the FOCs and the power cores remain valid.

5. Discussion

The work carried out by T. Kvarts and J. Karlstrand has clearly shown that the consequences of a break in the metallic parts of an FOC in a subsea cable are greatest where the metallic parts of the FOC have a low resistance and the sheath of the FOC is insulating. It is considered that the modelling carried out by both authors is appropriate and the conclusions are valid.

The higher the resistance of the metallic parts the lower the circulating current in the FOC and hence the less energy is available at any break in the FOC. Also, if the FOC has a semi-conducting sheath the leakage current through the sheath will reduce the circulating current and the voltage across any break in the metallic parts of the FOC.

To be effective the design of the FOC has to incorporate both high resistance metallic parts and a semi-conductive sheath. The work by T. Kvarts and J. Karlstrand and the supporting work conducted in this project has concluded that the resistivity of the semi-conductive cable sheath should not exceed 1000Ω·m at the operating temperature of the FOC. Cable standard IEC 60840 (IEC 60840: Power cables with extruded insulation and their accessories for rated voltages above 30 kV (Um = 36 kV) up to 150 kV (Um = 170 kV) - Test methods and requirements, 2011) contains maximum limits of 1000Ω·m and 500Ω·m for semi-conducting conductor and core screens, respectively, in power cables. Thus, suitable semi-conducting materials are readily available.

The author is aware of designs where a layer of insulating adhesive has been used between the metal tube and sheath of an FOC. Such a layer will increase the effective resistivity of the sheath and reduce the benefits of using a semi-conducting material. Clearly insulating adhesives should not be applied under the sheath of an FOC.

The work has shown that from the point of view of the risk of interaction between the FOC and the power cores the use of an FOC where the metallic part is a relatively high resistance stainless steel tube is preferred. This minimises the risk to a level where a power core failure would not be expected in the event of a break in the tube. However, use of an unarmoured tube may increase the risk of the tube breaking if the cable is subjected to excessive tension, over bending or other mishandling. Of the failures that have occurred several have been attributed to a break in a copper tube in the FOC which was assumed to be due to some form of mishandling. Also, it is known that unarmoured stainless steel tubes in FOC have failed, but the breaks are thought to have been found before the cables were energised.

The studies show that if an FOC has a stainless steel tube and stainless steel armour, combined with a sheath having a resistivity of no more than 1000Ω·m, the risk of a fault in the power cores due to a break in the FOC remains low. However, the temperature at the break may cause accelerated degradation of the sheath of the FOC which will accelerate the rate of water ingress to the fibres and hence the degradation in the performance of the optical fibres. With this design the risk of damage to the FOC, resulting in loss of fibres, is considered to be less than with an unarmoured FOC.

In subsea cables the FOCs are located in the interstices between the power cores and usually close to them. The modelling has shown that positioning the FOC closer to the armour has little

effect on the induced voltage. Positioning the FOC closer to the armour would make it less likely that heat generated at a break in the FOC would damage the power cores. However, this would move the FOC further from the axis of the cable and will increase the local mechanical stress on the FOC. Thus, the disadvantages of moving the FOC closer to the armour are likely to outweigh the advantages.

The review of AC corrosion of materials in seawater has shown that aluminium is very susceptible to such corrosion. Because of this, together with its relatively low resistance, aluminium should be avoided in FOCs included in subsea cables.

The papers covering AC corrosion of stainless steel have not provided definitive limits for the voltages and current densities that may lead to corrosion of stainless steel. However, they have indicated that corrosion may occur at current densities if the sheath of the FOC is damaged, where the sheath has a resistivity of greater than 1000Ω·m. This is supported by the paper by Gustavsen who reports that there has been a failure of a stainless steel tube in an offshore umbilical and the failure was attributed to AC corrosion. From the studies of FOC design it would not be expected that such a failure would occur or lead to a failure in a power core if the FOC has a sheath with a resistivity of less than 1000Ω·m. However, severe corrosion of the stainless steel tube in an FOC would lead to water ingress into the fibres and then loss of functionality of the fibres. Corrosion studies would be required to investigate the rate of corrosion that may occur in stainless steel due to damage to the sheath exposing a small area of stainless steel. Such a study is outside the scope of this report.

It is also clear that the metallic parts of an FOC must be earthed at both ends and earthed, or have continuity, at intermediate joints. Adequate earthing at intermediate joints can be achieved by providing continuity between the metallic parts of the FOC and the armour of the subsea cable. Where an FOC has armour and a stainless steel tube both parts should be earthed to avoid any standing voltage between them.

6. Conclusions

The studies described in this report have drawn heavily on two papers presented at Jicable 2019 by T. Kvarts and J. Karlstrand.

Both papers conclude that the use of FOCs having high resistance metallic parts, a stainless steel tube, combined with a sheath having a resistivity of no more than 1000Ω·m will minimise any risk of damage to the FOC leading to failure of the power cores. The studies carried out support this view.

An unarmoured design with a small diameter stainless steel tube would result in less heat being generated at any break in the FOC than an armoured design. However, an unarmoured design will have less mechanical strength and hence would be more susceptible to damage during manufacture, load-out and installation than an armoured design. Hence a design with stainless steel armour is proposed.

It is noted that irrespective of the design of the FOC any break in the metal tube water barrier will result in moisture ingress to the fibres. This will degrade the fibre performance. Thus, even if the fibres remain intact when the break occurs they will not remain functional for the expected life of the export cable.

It has been concluded that where the sheath of an FOC has a resistivity of no more than 1000Ω·m and the metallic parts consist of a small diameter stainless steel tube, to contain the fibres, and stainless steel wire armour the heat generated at a break in the FOC will not be sufficient to damage the power cores.

The possibility of AC corrosion of the stainless steel components has been considered. Published literature on AC corrosion is primarily concerned with AC corrosion of buried steel pipelines where there is a defect in the coating. The rate of corrosion is related to the current density at the defect. Thus, it is related to the driving voltage and the size of the defect. For a 1cm² defect in the sheath of an FOC, AC corrosion of the stainless steel would not be expected. However, corrosion testing with small defects/damage would be required to provide firm conclusions on the risk of AC corrosion in seawater.

It is concluded that all of the metallic parts of the FOC have to be earthed at both ends and be either earthed or made electrically continuous at any joints. Also, the use of an insulating adhesive between the metal parts and the sheath of the FOC must be avoided.

7. References

Benson, F. A., & Harrison, D. (1959). *Electric - Circuit Theory.* London: Edward Arnold Ltd.

(2013). *BS EN 15280 Evaluation of a.c. corrosion likelyhood of buried pipelines applicable to cathodically protected pipelines.* British Standards Institution.

French, W. H. (1973). *Alternating Current Corrosion of Aluminum.* IEEE Transactions on Power Apparatus and Systems PAS-92(6).

Gummrow, R. (1996). *IPC 1996 - 1849: AC Corrosion - A new threat to pipeline Integrity.* International pipeline conference.

Gustavsen, B. (2018). *Voltages and AC Corrosion on Metallic Tubes in Umbilical Cables Caused by Magnetic Induction From Power Cable Charging Currents,.* IEEE Transactions on Power Delivery PP(99):1.

(2011). *IEC 60840: Power cables with extruded insulation and their accessories for rated voltages above 30 kV (Um = 36 kV) up to 150 kV (Um = 170 kV) - Test methods and requirements.* IEC.

Karlstrand, J. (2019). *Electromagnetic coupling in HV and EHV three-core submarine cables during test and operation.* Jicable.

Kvarts, T. (2019). *Inherently safe designs of fibre optic cables integrated in three-core submarine power cables.* Jicable.

Luoni, G., & Anelli, P. (1976). *Armour corrosion in single core submarine AC cables.* IEEE PES Symposium.

(1995). *TB 95 - Guide to the influence of high voltage AC power systems on metallic pipes.* CIGRE.

Wedmore, E. B. (1930). *Heating of buried cables - Alleviation of loacl heating by thermal conduction lengthwise - F/T33.* British Electrical and Allied Industries Research Association .

The Carbon Trust is a company limited by guarantee and registered in England and Wales under Company number 4190230 with its Registered Office at: 4th Floor, Dorset House, 27-45 Stamford Street, London SE1 9NT.

Published in the UK: 2021.